

Supporting Information¹

An *in situ* gas chromatograph with automatic detector switching between Vocus PTR-TOF-MS and EI-TOF-MS: Isomer resolved measurements of indoor air

Megan S. Claflin¹, Demetrios Pagonis^{2,3}, Zachary Finewax^{2,3,4}, Anne V. Handschy^{2,3}, Douglas A. Day^{2,3}, Wyatt L. Brown^{2,3}, John T. Jayne¹, Douglas R. Worsnop¹, Jose L. Jimenez^{2,3}, Paul J. Ziemann^{2,3}, Joost de Gouw^{2,3}, Brian M. Lerner¹

¹ Aerodyne Research Inc., Billerica, Massachusetts 01821, United States

² Cooperative Institute for Research in Environmental Sciences (CIRES), Boulder, Colorado 80309, United States

³ Department of Chemistry, University of Colorado, Boulder, Colorado 80309, United States

⁴ Now at Chemical Sciences Laboratory, Earth System Research Laboratory, National Oceanic and Atmospheric Administration, Boulder, Colorado, 80305, United States

Correspondence to: Megan S. Claflin (mclaflin@aerodyne.com)

Monoterpene calibration curves for GC-EI-TOF and GC-Vocus; monoterpene chromatogram by GC-Vocus; Allan variance plot of RT-Vocus data; monoterpene timeseries by GC-EI-TOF; RT-Vocus detection of C₁₀H₁₇⁺ in the room versus supply air during elevated emission events; chromatogram, electron ionization mass spectrum, high resolution fitting, and time series of dimethylsilanediol.

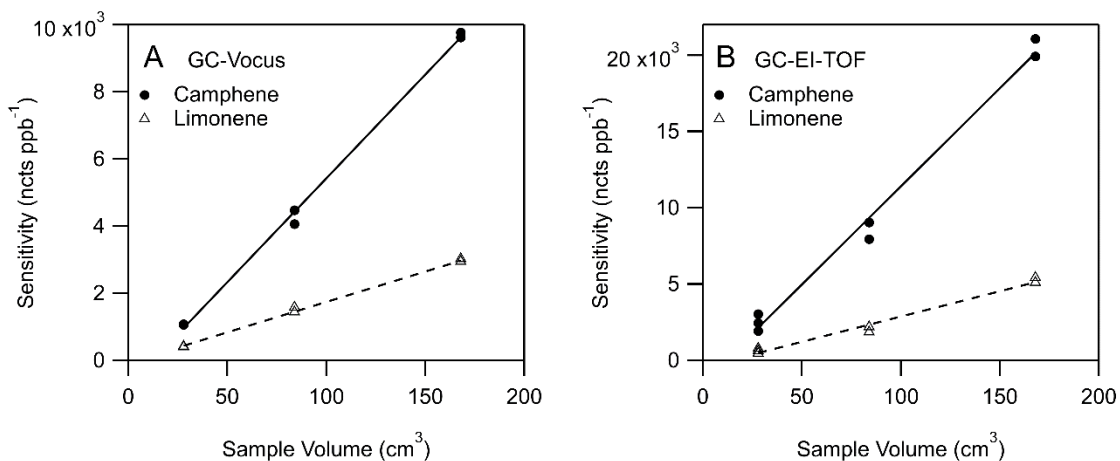


Figure S1. Monoterpene sensitivities (normalized counts per ppb) versus sample volume for limonene and camphene acquired by A) GC-Vocus and B) GC-EI-TOF. Monoterpenes were quantified using their protonated molecular ion ($C_{10}H_{17}^+$) for GC-Vocus, and characteristic fragment ion ($C_7H_9^+$) for GC-EI-TOF.

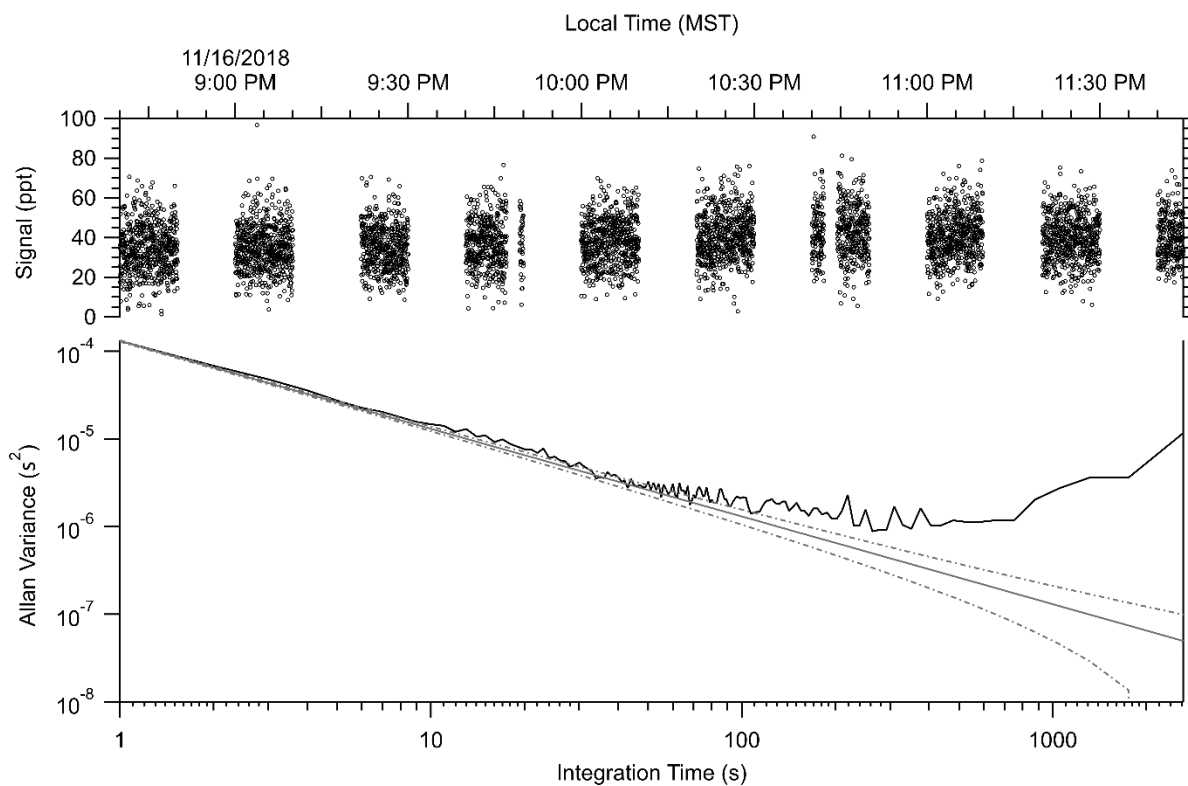


Figure S2. Allan variance plot of the RT-Vocus $C_{10}H_{17}^+$ signal. The RT-Vocus trace contains only room air measurements, periods of sampling from the supply air were removed. The subset of $C_{10}H_{17}^+$ signal was chosen when the concentration was both low and contained minimum perturbations from local sources. The Allan variance analysis results in a minimum at ~ 250 s of averaging time, meaning that if the RT-Vocus data was averaged to give one data point every 250 s the noise could be reduced by a factor of ~ 16 .

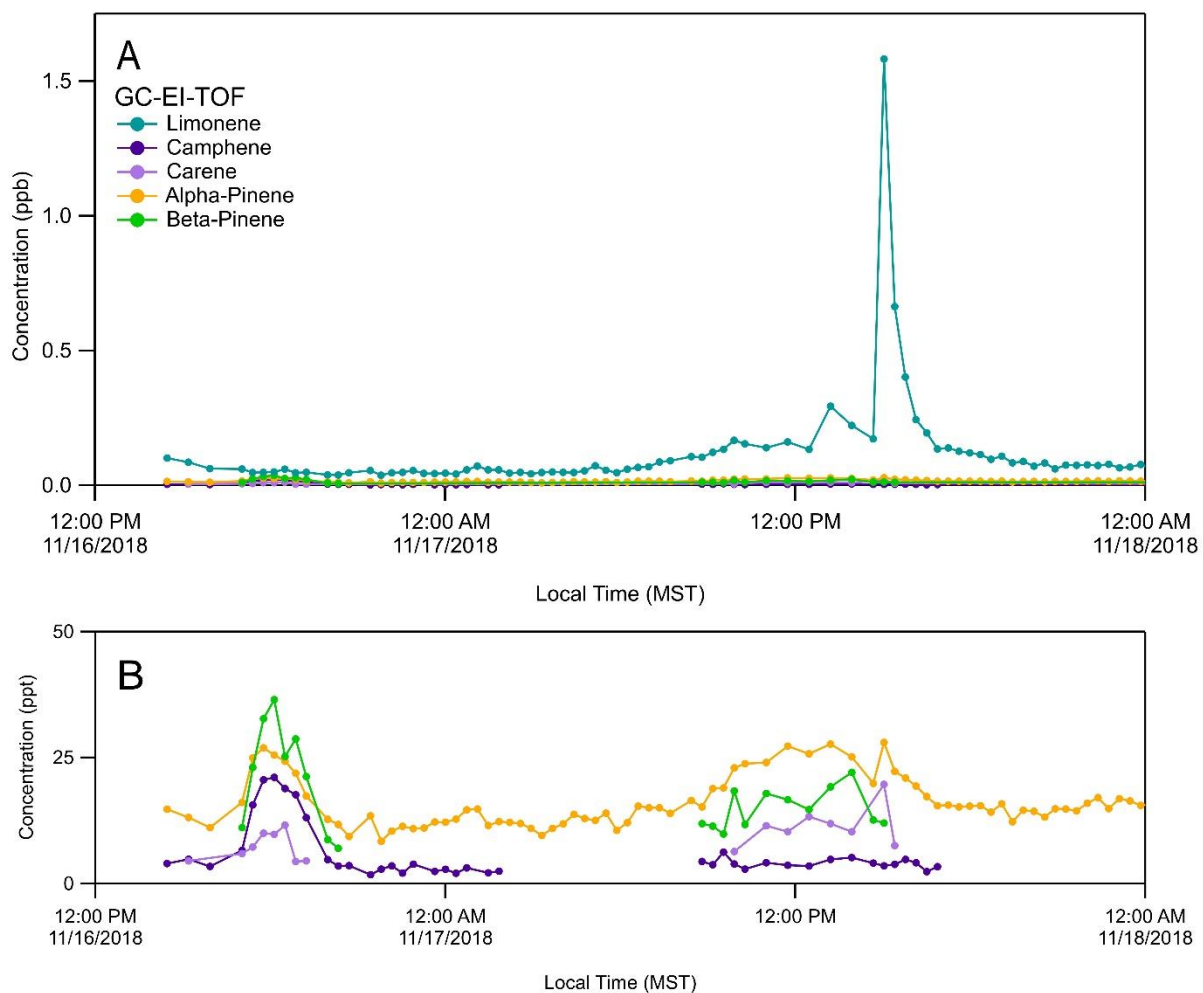


Figure S3. (A) GC-EI-TOF monoterpene time series (B) details of monoterpenes detected in lower ambient concentrations, absent data points are for chromatograms where the chromatographic peak was below the limit of detection. Large peak in limonene on November 17 is due to enhancements observed after the football game, while the increase in signal for the other monoterpenes on November 16 is associated with the inflow of outdoor air into the room.

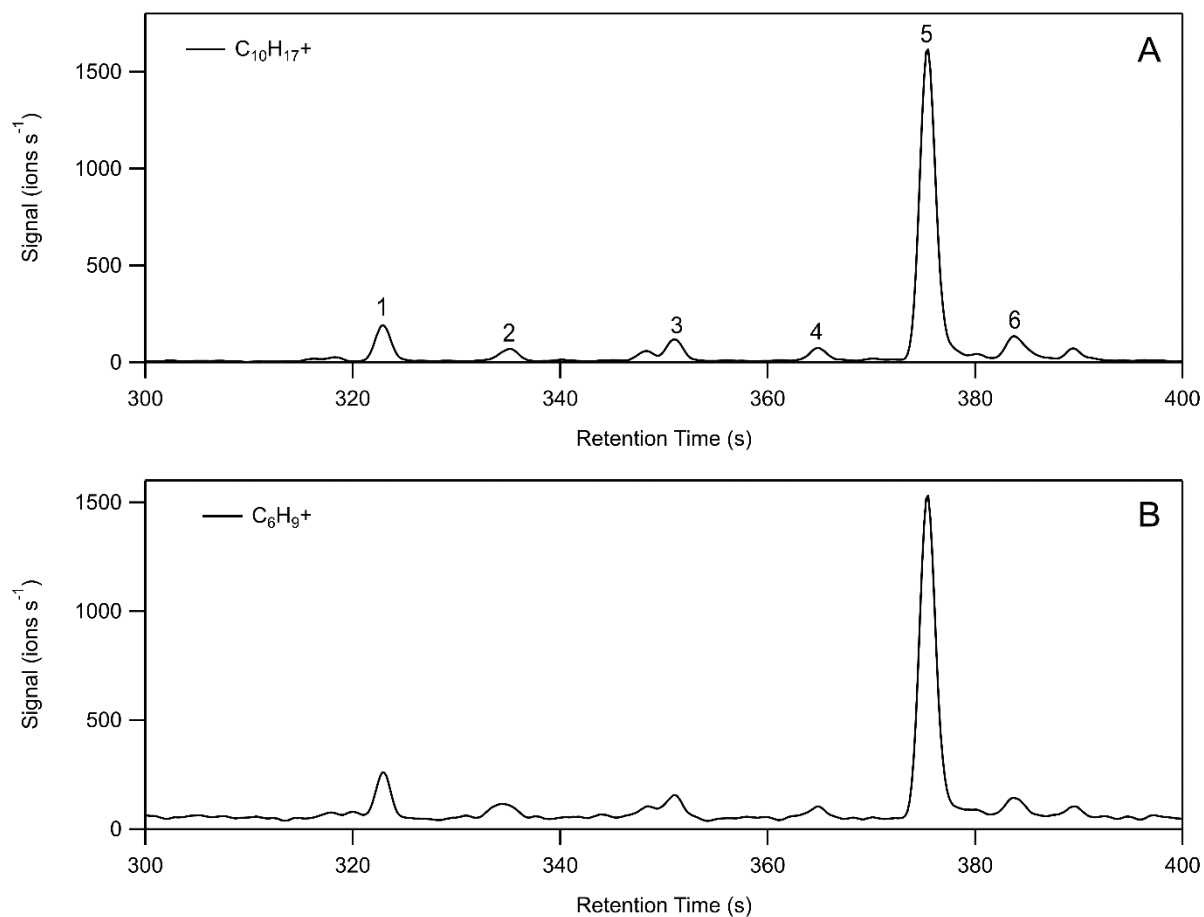


Figure S4. Ambient GC-Vocus chromatogram, showing subsection of the chromatogram where the monoterpenes elute, demonstrating separation of Vocus signal (A) C₁₀H₁₇⁺ (m/z 137.1325), the protonated molecular ion of monoterpenes where peaks labeled 1 – 6 correspond to α -pinene, camphene, β -pinene, carene, limonene, and γ -terpinene, respectively, and (B) C₆H₉⁺ (m/z 81.0699) ion being detected here as fragmentation ions of the monoterpenes.

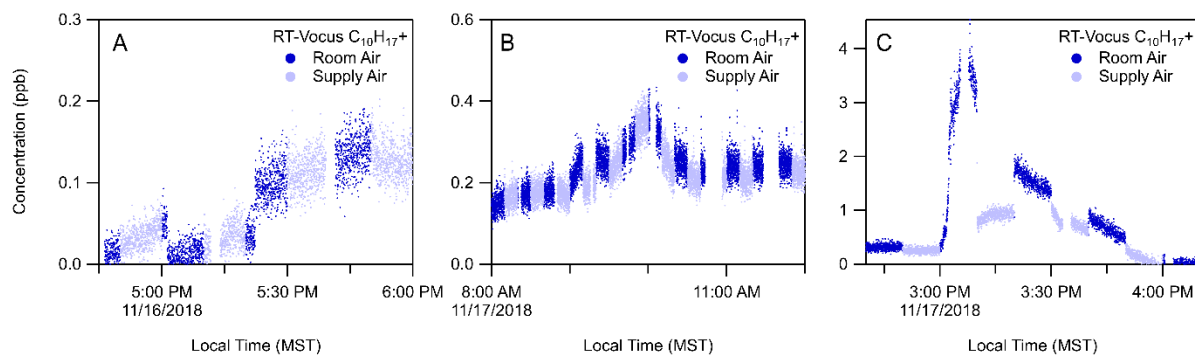


Figure S5. RT-Vocus detection of $C_{10}H_{17}^+$ during A) elevation increase on November 16, initially observed in the supply air indicating an outdoor source of biogenics B) the tailgating and football game event on November 17 where both the room and supply air showed similar elevated signals indicating a source in close proximity to the weight room and C) elevation increase after the football event on November 17, where the increase in signal was initially detected in the room air at 3 pm, followed by subsequent increase in the supply air, indicating an in-room source of monoterpene emissions.

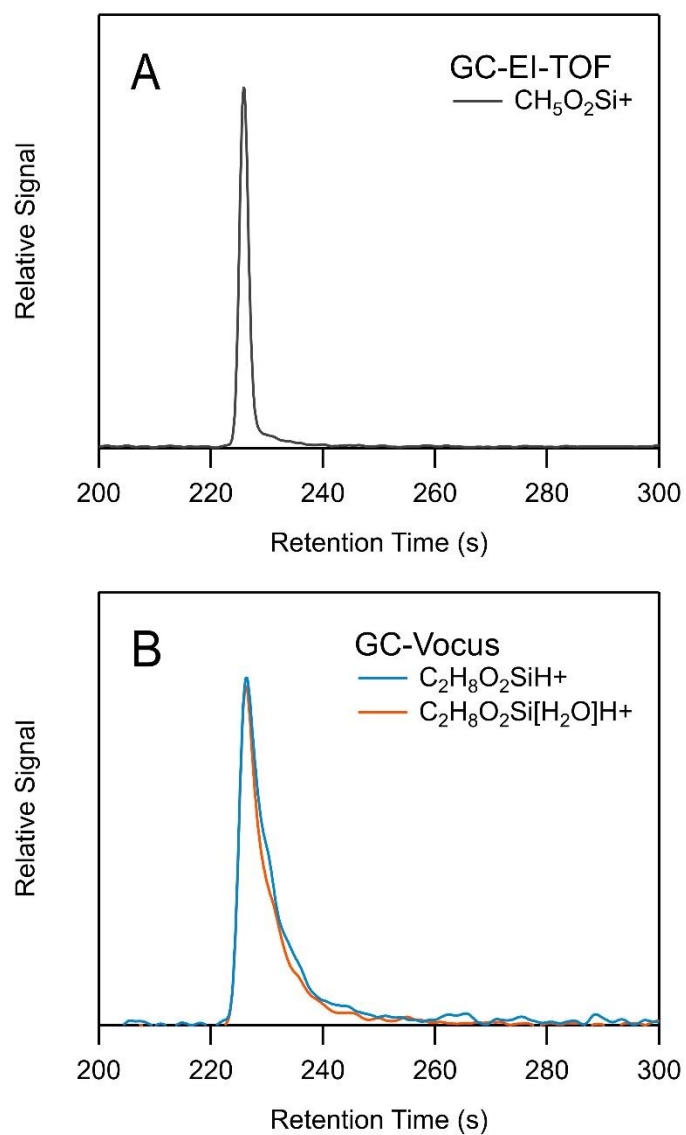


Figure S6. Chromatographic separation of DMSD with retention time 230 s (A) GC-EI-TOF detection of DMSD characteristic ion $\text{CH}_5\text{O}_2\text{Si}^+$ (B) GC-Vocus detection of both the protonated molecular ion, $\text{C}_2\text{H}_8\text{O}_2\text{SiH}^+$, and its water cluster, $\text{C}_2\text{H}_8\text{O}_2\text{Si}[\text{H}_2\text{O}]\text{H}^+$.

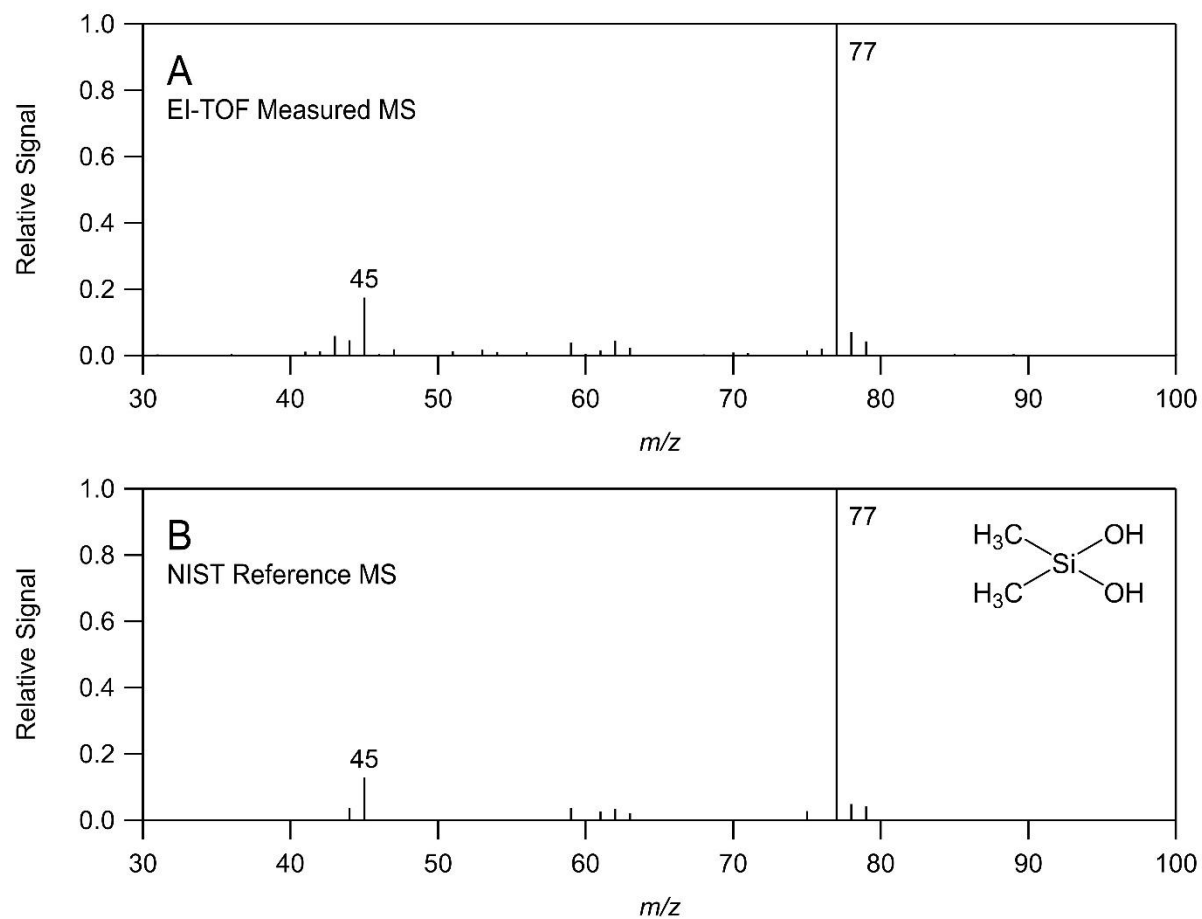


Figure S7. Electron ionization mass spectrum of DMSD for (A) chromatographic peak obtained by GC-EI-TOF and (B) standard NIST mass spectrum.

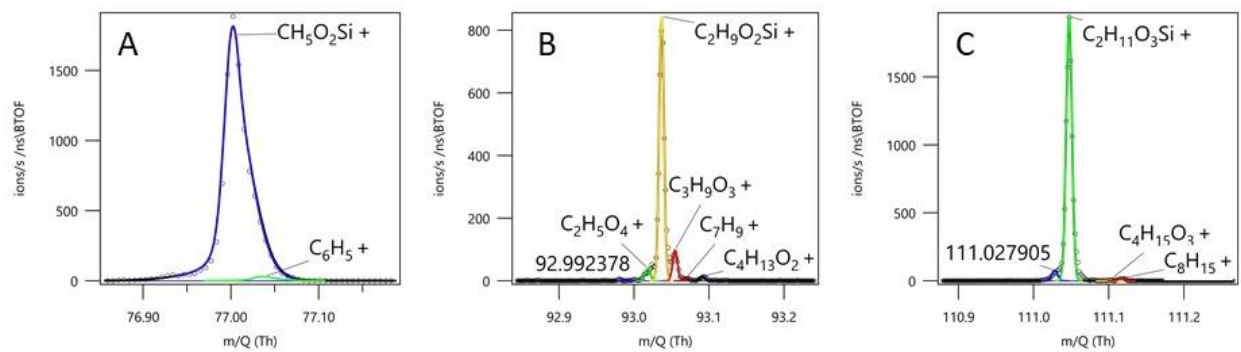


Figure S8. Mass spectrum high resolution peak fits of DMSD during chromatographic separation (A) characteristic fragmentation ion, $\text{CH}_3\text{O}_2\text{Si}^+$, detected by EI-TOF (B) protonated molecular ion, $\text{C}_2\text{H}_8\text{O}_2\text{SiH}^+$, and (C) its water cluster, $\text{C}_2\text{H}_8\text{O}_2\text{Si}[\text{H}_2\text{O}]\text{H}^+$, detected by Vocus.

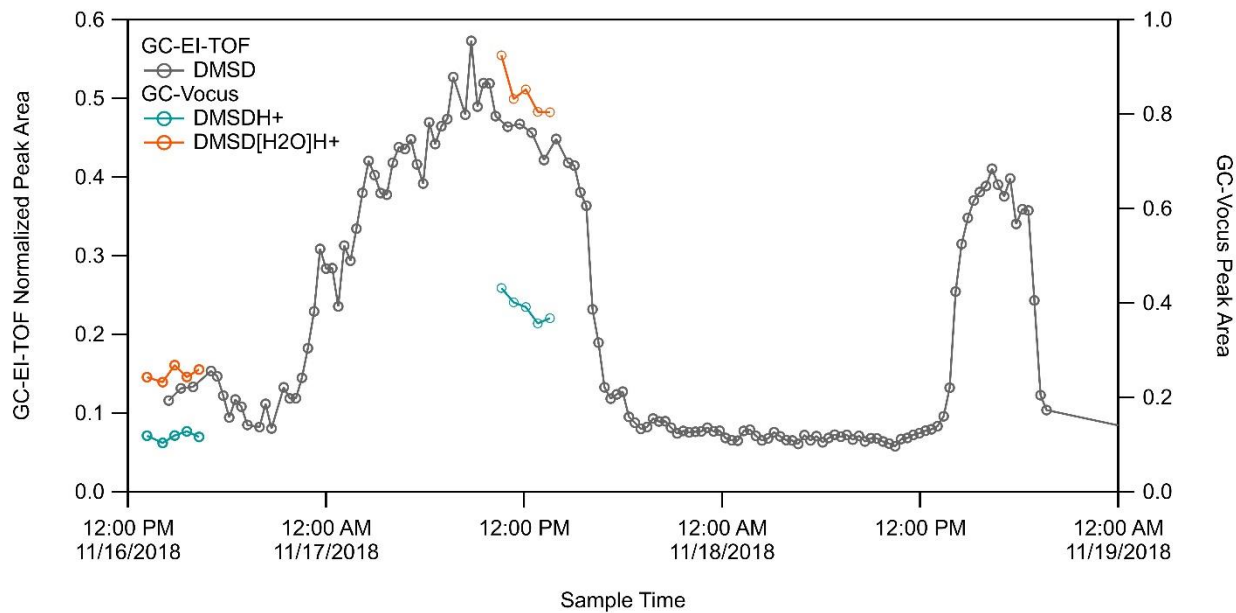


Figure S9. Time series of DMSD detected by GC-EI-TOF (grey trace) and GC-Vocus (blue trace, protonated molecular ion; orange trace, water cluster of protonated molecular ion).